Bull. Mater. Sci., Vol. 12, Nos 3 & 4, September 1989, pp. 369–379. © Printed in India.

A cold model study of mass transfer in Q-BOP

N PRASAD, S SINGH and S L MALHOTRA

Department of Metallurgical Engineering, Institute of Technology, Banaras Hindu University, Varanasi 221 005, India.

Abstract. At steel-making temperature, chemical kinetics can rarely be the rate-limiting step. Thus most of the reactions are limited by the rate of mass transfer to and from the reaction interface. The overall rate of mass transfer may be controlled by gas phase mass transfer or liquid phase mass transfer. Since in Q-BOP, the rate of reaction may be controlled by the rate of mass transfer in gas phase or in liquid phase, both were studied in a cold model. The different variables studied were tuyere diameter, jet direction, flow rate of gas and tuyere depth. The results of gas phase mass transfer indicate that the effect of tuyere diameter and jet direction is very small. For Reynolds number less than 9000 the effect of flow rate and tuyere depth is given by the equation, $K_g A/L_0 Q = 0{\cdot}02 d_0 + 0{\cdot}043$, whereas for Reynolds number greater than 9000 the effect of flow rate and tuyere depth is given by the equation, $K_g A/L_0 Q = 0{\cdot}061 d_0 + 0{\cdot}046$. Similarly the liquid phase mass transfer coefficient is independent of the tuyere diameter and the shrouding gas, and is not much affected by the jet direction. The effect of gas flow rate and tuyere depth is given by the equation, $K_L A = 0{\cdot}077 (Q)^{0{\cdot}75} (L_0)^{0{\cdot}61}$.

Keywords. Mass transfer; cold model; Q-BOP.

1. Introduction

Refining of liquid pig iron to steel using gaseous oxygen shrouded by a hydrocarbon is well-established. The different names used for this process are Q-BOP, OBM, LWS and SIP. For the sake of consistency, the term Q-BOP will be used throughout the present text. Our understanding of the process is inadequate. The physical picture of the flow of gas through the liquid is quite complicated and not very clear. Reactions between a submerged gas jet and a liquid occur at the gas jet and liquid interface. At steel-making temperatures, chemical kinetics can rarely be the rate-limiting step. Thus most of the reactions are limited by the rates of mass transport processes to and from the reaction interface. The mass transfer to the gas-liquid interface from the metal and gas phases maintains the supply of the reactants and removal of the products. In case the mass transfer from the gas phase is very slow and determines the overall reaction rate, the reaction is termed gas-phase mass transfer controlled. Similarly whenever the mass transfer from the liquid phase is the rate-controlling step, the reaction is termed liquid-phase mass transfer controlled. Both gas-phase mass transfer controlled as well as liquid-phase mass transfer controlled reactions are operative in Q-BOP (Brotzmann *et al* 1976; Fruehan 1976).

With the objective of improving the understanding of the process, mass transfer studies were carried out in a room temperature model to know the effect of operating parameters on the rate of refining. Both, gas-phase and liquid-phase controlled mass transfer were studied. In Q-BOP steel-making the jet enters the melt as a bubble column. As the bubble column rises, it splits into small bubbles. The actual bubble

formation at the tuyere is very complex. It is almost impossible to determine the interfacial area between gas and liquid. It is easier to measure the combined product of mass transfer coefficient and interfacial area as a function of the operating variables. In this study, the product of mass transfer coefficient, K, and interfacial area A, has been called volumetric mass transfer coefficient, KA.

2. Experimental set-up

A layout of the set-up is schematically shown in figure 1. It consists of a simulating vessel and two gas-flow lines representing a reactive gas and a shrouding gas. The air-flow line consists of an air compressor, flow regulating valves, a calibrated rotameter, an air filter, a chamber for temperature measurement and a mercury manometer. The carbon dioxide flow line consists of a carbon dioxide cylinder, flow regulating valve, a rotameter, a chamber for temperature measurement and a manometer. A cylindrical perspex container of 54·7 cm internal diameter and 63 cm height is used as the vessel. Five holes are drilled and threaded at the bottom of the vessel for fitting the tuyeres. One hole is located at the centre of the bottom and the remaining four in one half of the bottom, arranged in the form of an arc of a circle of 13·7 cm radius. The holes not in use are closed with rubber bungs.

In the case of gas-phase mass transfer study there is a slight modification in the experimental set-up. A needle valve is inserted in the carbon dioxide flow line for fine control of the flow. The rotameter is replaced with a soap bubble flowmeter for measuring the flow rate of carbon dioxide. Carbon dioxide and air are mixed with each other before entry into the gas filter containing glass wool.

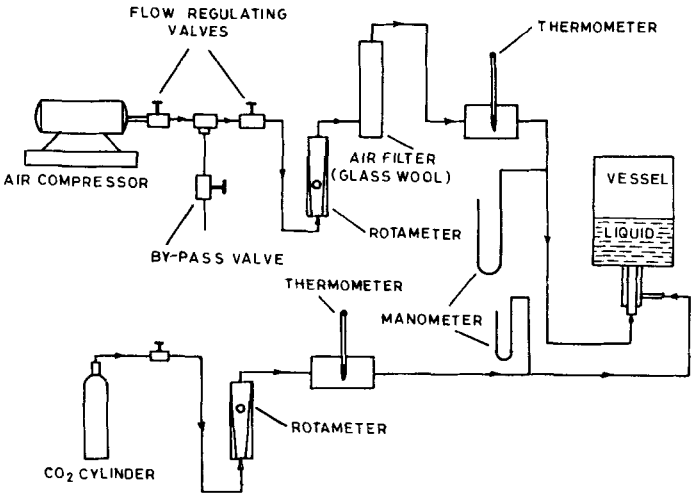

Figure 1. Schematic diagram of the experimental set-up.

3. Gas-phase mass transfer

$NaOH–CO_2$ system was chosen for this study. The choice was verified experimentally by blowing 1% CO_2 mixed with air into a liquid bath containing 0·15 mol/l NaOH. It is observed that the mass transfer in the gas phase controls the reaction rate until the concentration of NaOH reduces to about 0·017 mol/l. The experimental conditions are listed in table 1.

41,000 cm^3 of 0·15 mol/l NaOH solution were transferred to the vessel, through which was blown a 1% CO_2–air mixture. The change in the CO_2 content of the bath is so slow that a pH meter can not be used to monitor it. Hence samples were obtained at regular intervals and titrated for the CO_2 content. The sampling position was generally 10 cm from the jet axis at half the tuyere depth. However, the CO_2 content is observed to be independent of the sampling position. The rate controlled by gas phase mass transfer is represented by the equation (Brotzmann *et al* 1976)

$$K_g A = -Q\,Ln(P^B_{CO_2}/P^0_{CO_2}). \tag{1}$$

$P^B_{CO_2}$ was calculated using the equation (Brotzmann *et al* 1976),

$$P^B_{CO_2} = P^0_{CO_2} - (mV_b RT/Q). \tag{2}$$

Table 1. Experimental conditions.

Studies	Gas-phase mass transfer $NaOH–CO_2$ system	Liquid phase mass transfer $NaOH–CO_2$ system	Liquid phase mass transfer water–CO_2 system
Vessel diameter, D(cm)	54·7	19·8	54·7
Bath liquid	0·15 mol/l NaOH-solution	0·05 mol/l NaOH-solution	Water
Bath height, L_b(cm)	17·5	7·2	19·2
Jet gas	1% CO_2 in air	Carbon dioxide	Carbon dioxide
Jet gas flow rate (cm^3/s)	50 to 1200	25 to 200	25 to 600
Shrouding gas	—	Air	—
Shrouding gas/ jet gas ratio	—	0·1	—
Tuyere diameter, d_0(cm)	0·159, 0·318 0·476, 0·635	0·318	0·159, 0·318, 0·635
Tuyere depth L_0(cm)	6–15 cm	1–7 cm	1–5 cm
Annulus thickness (cm)	—	0·1	—
Thickness of the wall of the inner pipe (cm)	—	0·12	—
Number of tuyeres	1	1	1, 3, 5
Jet direction	Bottom-blown, horizontal and top-blown submerged jets	Bottom-blown	Bottom-blown, horizontal and top-blown submerged jets

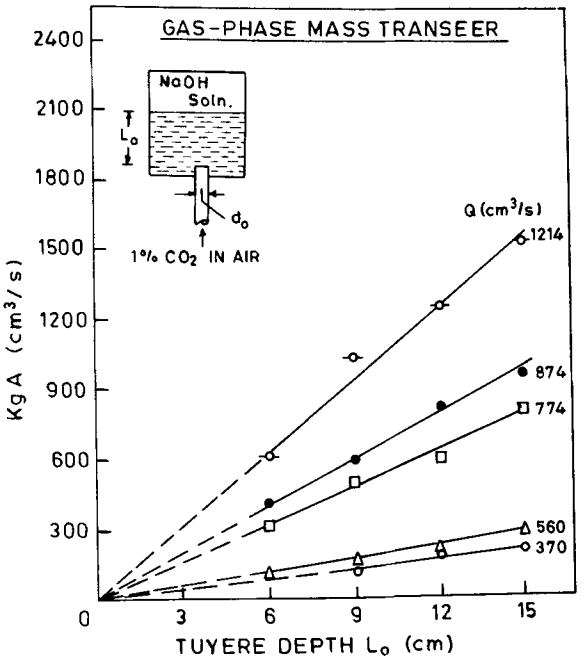

Figure 2. Effect of tuyere depth on the gas-phase volumetric mass transfer coefficient (K_gA).

The value of A and K_g cannot be separated by mass transfer studies alone and have been reported as a single parameter in the present work. K_gA has been termed the volumetric gas phase mass transfer coefficient. The effect of tuyere depth, gas flow rate, tuyere diameter and direction of the submerged jet were studied. The effect of tuyere depth on K_gA is shown in figure 2. K_gA increases linearly with tuyere depth over the range studied. For a given tuyere diameter and flow rate, the bubble characteristics and thus the gas phase mass transfer coefficient (K_g) in the bubbles may be considered as remaining constant. Thus the results indicate that the interfacial area between the gas bubbles and liquid is proportional to the tuyere depth. The effect of gas flow rate on K_gA/L_0 for different tuyere diameters is shown in figure 3. K_gA/L_0 increases with flow rate, but d_0 does not seem to have any significant effect. Figure 3 also indicates that there are two regions, the transition point being at about 500 cm^3/s of gas flow rate ($N_{Re} = 9000$). The effect of d_0 in both the regions is given by the following empirical relations.

(a) For $N_{Re,0}$ less than 9000,

$$K_gA/L_0Q = 0{\cdot}02d_0 + 0{\cdot}043. \tag{3}$$

(b) For $N_{Re,0}$ greater than 9000,

$$K_gA/L_0Q = 0{\cdot}061d_0 + 0{\cdot}046. \tag{4}$$

Some experiments were conducted with horizontal and top blown submerged jets in order to compare their behaviour with that of bottom blown jets. The results are plotted in figure 4. The value of K_gA is minimum for top-blowing. Visual observation established that the break of the jet into bubbles was less for top-blowing as compared

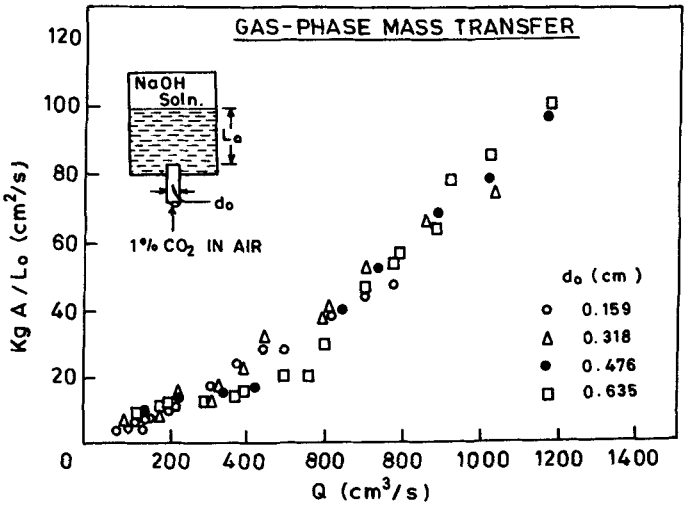

Figure 3. Effect of gas flow rate and tuyere diameter on K_gA/L_0.

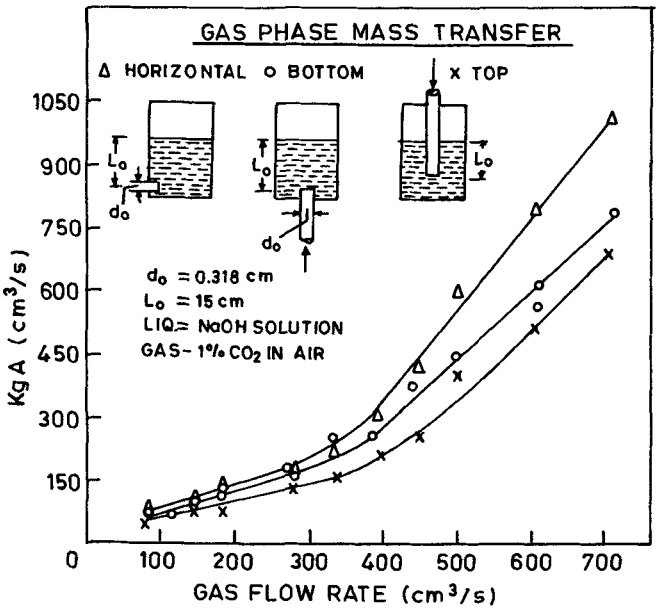

Figure 4. Effect of jet direction on the gas-phase volumetric mass transfer coefficient (K_gA).

to bottom-blowing resulting in lower surface area and thus lower K_gA for the top-blowing. Side-blown jets have higher values of K_gA as compared to the bottom-blown ones due to the increase in the length of the trajectory of the jet.

A plot of K_gA/L_0 against gas flow rate for the bottom-blown and horizontal jets is shown in figure 5. For horizontally injected gas jets, Brimacombe *et al* (1974) have plotted dimensionless jet trajectory length (S/d_0) vs dimensionless vertical distance from tuyere exit (X/d_0) using the theoretical expression derived by Themelis *et al* (1976). In the present work this plot has been used to calculate the jet trajectory length of horizontal jets. As shown in figure 5, the values of K_gA/L_0 for both the

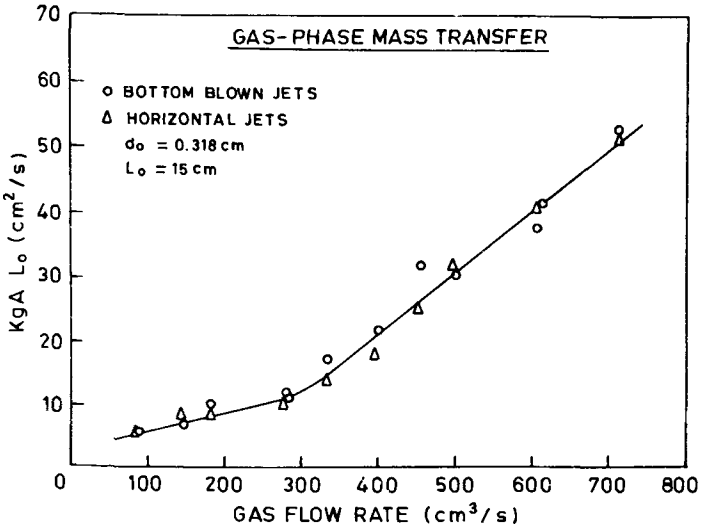

Figure 5. Effect of horizontal- and bottom-blown jets on K_gA/L_0.

bottom-blown and horizontal submerged jets are identical. This indicates that the higher values of K_gA/L_0 obtained for horizontally injected jets as compared to the bottom-blown jets in the present work are due to increased trajectory length and hence the gas/liquid interfacial area.

4. Liquid-phase mass transfer

The two systems used were NaOH–CO_2 and water–CO_2. The NaOH–CO_2 system was used to study the effect of shrouding the reactive gas jet on the liquid phase mass transfer. Air was used as the shrouding gas. It was observed that there is no effect of shrouding the gas jet on the liquid phase mass transfer. For further work, the set-up was simplified by replacing the NaOH–CO_2 system with a water–CO_2 system and no shrouding gas was used. The experimental conditions for both the systems are listed in table 1.

The values of K_LA were calculated by using the relation,

$$Ln[(C_e - C_t)/(C_e - C_0)] = -(K_LAt/V_b). \tag{5}$$

Equation (5) is a standard relation used in convective mass transfer for calculating K_LA (Inada and Watanabe 1977; Fruehan and Martonik 1978; Bradshaw and Chatterjee 1971).

4.1 *The NaOH–CO_2 system*

2200 ml of 0·05 mol/l NaOH solution was transferred to a vessel, and its temperature was maintained at 25°C. Blowing in of air and CO_2 at predetermined rates was started. The changes in pH were recorded at intervals of 1 min. The pH electrodes were usually kept at 5 cm from the centre of the jet. However, the pH of the solution was observed to be independent of the position of electrode in the solution.

The relationship given by Inada and Watanabe (1977) was applied for preparing a calibration curve of pH vs. CO_2 content for 0·05 mol/l NaOH solution. This curve was used to read the CO_2 concentration in the bath corresponding to the recorded pH.

Two sets of experiments were performed by varying the flow rates of CO_2 and the tuyere depths. In the first set no shrouding gas was used while in the second set air was used to shroud the CO_2 jet. The flow rate of air was kept at 10% of the flow rate of CO_2. The effect of shrouding the jet on $K_L A$ at different tuyere depths and at different flow rates of reactive gas is shown in figure 6. It is clear from the figure that there is no effect of shrouding the gas on $K_L A$. This observation suggests that the shrouding gas does not provide any physical shield.

4.2 *Water–CO_2 system*

Water (45,000 cm^3) was transferred to a 54·7 cm diameter vessel. The pH of water used was usually 7·5 but if less than 7·5 was adjusted by bubbling a small amount of nitrogen into the bath. Blowing of CO_2 was started at the required flow rate. Bath samples were withdrawn at regular intervals and their pH values measured. The CO_2 concentration was read from the experimentally determined calibration curve between pH and CO_2 concentration. The effect of variables such as tuyere diameter, gas flow rate, tuyere depth, number of tuyeres and direction of the jet on the liquid phase mass transfer was studied.

The effect of tuyere diameter on $K_L A$ is shown in figure 7. It is evident that $K_L A$ is independent of tuyere diameter over the entire range studied. The Reynolds number of the jet varies from about 700 to 50,000. From the limited understanding about the formation of bubbles in submerged jets it appears that the bubble or cone after detachment from the orifice breaks into smaller bubbles. The size of the smaller bubbles thus formed is independent of the conditions at the nozzle (Sahai and Guthrie 1982; McNallan and King 1982). The recirculation of liquid is also not influenced by hydrodynamic conditions at the nozzle (Sahai and Guthrie 1982). It is thus expected

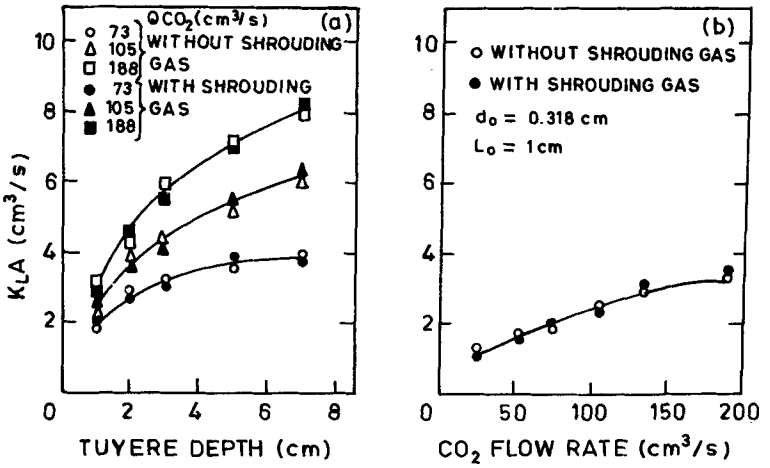

Figure 6. Effect of shrouding the jet gas on the volumetric mass transfer coefficient ($K_L A$), (a) at different tuyere depth, (b) at different CO_2 flow rates (liquid–NaOH solution, jet gas–CO_2, shrouding gas–air).

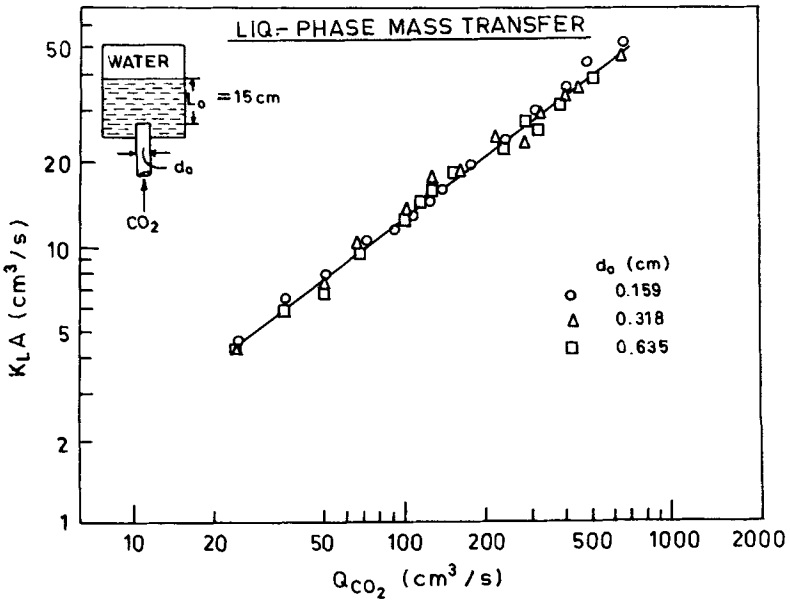

Figure 7. Effect of gas-flow rate and tuyere diameter on the liquid-phase volumetric mass transfer coefficient ($K_L A$).

that the liquid phase mass transfer rate is independent of the nozzle diameter as indicated by the results of the present study. The effect of gas flow rate on $K_L A$ is also shown in figure 7 and that of tuyere depth in figure 8. $K_L A$ increases with flow rate and tuyere depth. The empirical relationship obtained for the effect of flow rate and tuyere depth is given by

$$K_L A = 0{\cdot}077(Q_{CO_2})^{0{\cdot}75}(L_0)^{0{\cdot}61}. \tag{6}$$

A similar relationship obtained by Fruehan and Martonik (1978) is given by,

$$K_L A = 0{\cdot}088(Q_{CO_2})^{0{\cdot}75}(L_0)^{0{\cdot}69}. \tag{7}$$

and that derived from the work of Inada and Watanabe (1977) is given by

$$K_L A = 0{\cdot}466(Q_{CO_2})^{0{\cdot}65}. \tag{8}$$

Thus the relationship obtained in the present study is in good agreement with results obtained by the two groups of investigators indicated above. The liquid-phase mass transfer increases with flow rate because the number of bubbles and thus the gas/liquid interface increases. The liquid-phase mass transfer also increases with tuyere depth because the retention time of an individual bubble is increased.

The effect of number of tuyeres on $K_L A$ is shown in figure 9. The number of tuyeres used were 1, 3 and 5. The tuyeres were placed quite a distance apart so that there was no overlapping of the jets. Figure 9 shows that increase in the number of tuyere reduces the value of $K_L A$ per tuyere but total $K_L A$ is independent of the number of tuyeres. This is in agreement with the results of a cold model study by Inada and Watanabe (1977). Claes and Dauby (1978), on the basis of results from a 150 ton

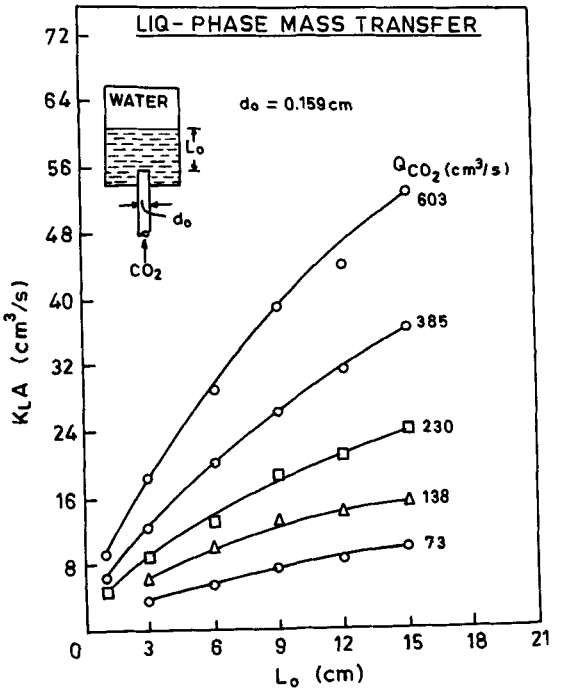

Figure 8. Effect of tuyere depth (L_0) on the liquid-phase volumetric mass transfer coefficient ($K_L A$).

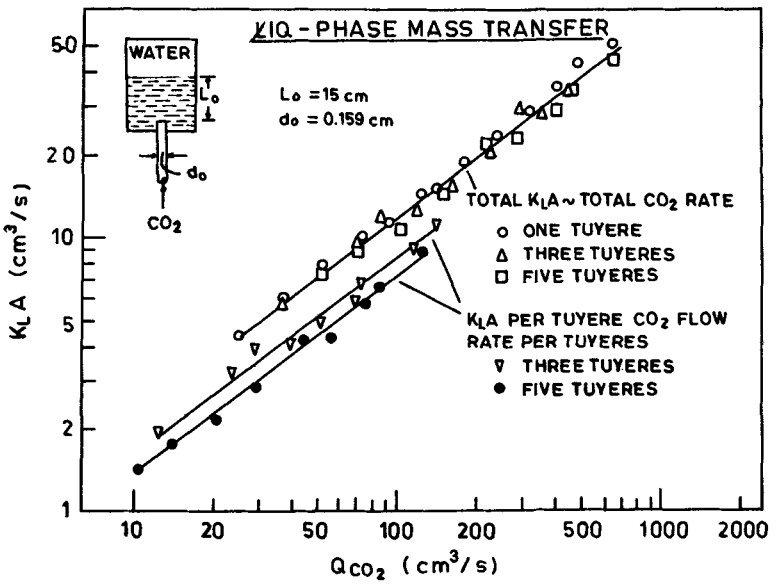

Figure 9. Effect of number of tuyere on the liquid-phase volumetric mass transfer coefficient ($K_L A$).

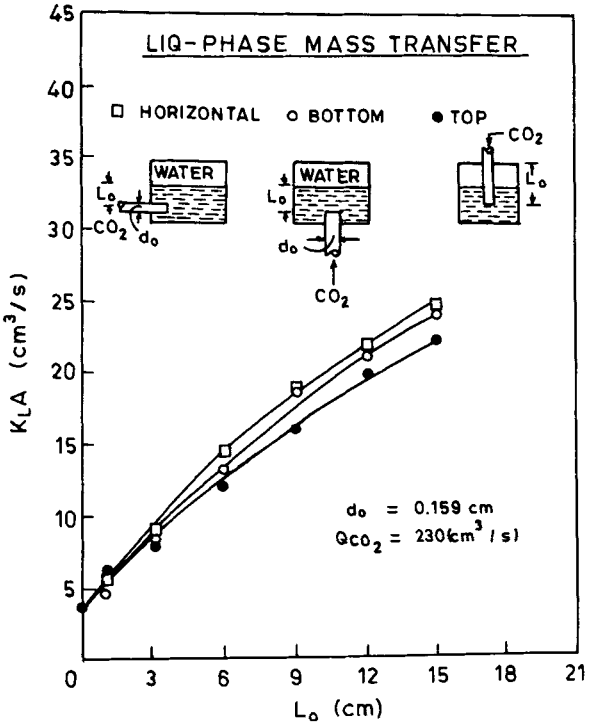

Figure 10. Effect of direction of the submerged jets on the liquid-phase volumetric mass transfer coefficient ($K_L A$).

converter also concluded that the number of tuyeres does not influence the kinetics of chemical reaction. The effect of jet direction on $K_L A$ is shown in figure 10. The jet direction in increasing order of $K_L A$ is top-blown, bottom-blown and horizontal-blown. However the difference in the values of $K_L A$ as a function of jet direction is very small.

Fruehan (1976) on the basis of results of nitrogen pick-up in 30 ton Q-BOP estimated the interfacial area and the liquid-phase mass transfer coefficient to be $1{\cdot}1 \times 10^6$ cm^2 and 0·03 cm/s respectively. Thus the value of $K_L A$ for the system was $3{\cdot}3 \times 10^4$ cm^3 s. The static bath depth was 76 cm which increased to 100 cm when blowing 0·7 m^3/s of nitrogen. Substitution of the data in (6) of the present work gives $K_L A = 3{\cdot}0 \times 10^4$ cm^3 s. The above figure estimated from the present work is in good agreement with the value obtained from Fruehan's (1976) work under actual process conditions.

5. Conclusions

(i) Both $K_g A$ and $K_L A$ increase with increase in flow rate and tuyere depth. The effect of these variables is less for $K_L A$ as compared to $K_g A$. $K_g A$ is a very weak function of tuyere diameter.

(ii) Jet direction, both in order of increasing $K_g A$ and $K_L A$, is top-blown, bottom-blown and horizontal-blown. However, the differences are not large.

(iii) The use of shrouding gas does not affect the value of $K_L A$.
(iv) The calculated value of $K_L A$ for Q-BOP using the equation obtained from the present study is in agreement with the estimated value under actual operating conditions.

List of symbols

A surface area of the interface, cm^2;
C_e equilibrium concentration, $mol\,cm^{-3}$;
C_0 initial concentration, $mol\,cm^{-3}$;
C_t concentration after t s, $mol\,cm^{-3}$;
d_0 tuyere diameter, cm;
K_g gas-phase mass transfer coefficient, $cm\,s^{-1}$;
K_L liquid phase mass transfer coefficient, $cm\,s^{-1}$;
L_0 tuyere depth (liquid height above the tuyere exit), distance along jet trajectory, cm;
m slope of the plot: CO_2 content vs. time, $mol\,cm^{-3}\,s^{-1}$;
N_{Re} Reynolds number, dimensionless;
$P^B_{CO_2}$ partial pressure of CO_2 in the gas at the bath surface, atm;
$P^0_{CO_2}$ partial pressure of CO_2 at the tuyere orifice, atm;
Q volumetric flow rate of the gas, $cm^3 s^{-1}$;
Q_{CO_2} volumetric flow rate of CO_2, $cm^3 s^{-1}$;
R gas constant, $82{\cdot}1\,cm^3\,atm\,mol^{-1}\,K^{-1}$;
T temperature, K;
t time, s;
V_b bath volume, cm^3.

References

Bradshaw A V and Chatterjee A 1971 *Chem. Eng. Sci.* **26** 676
Brimacombe J K, Stratigakas E S and Tarasoff P 1974 *Metall. Trans.* **5** 763
Brotzmann K, Lankfort W T Jr and Brisse A H 1976 *Iron making and steel making* **3** 259
Claes J R and Dauby P H 1978 Third International Iron and Steel Congress (Conf. Proc.) Chicago, Illinois, 512
Fruehan J R 1976 *Iron making and steel making* **3** 33
Fruehan J R and Martonik L J 1978 Third International Iron and Steel Congress (Conf. Proc.), Chicago, Illinois, 229
Inada S and Watanabe T 1977 *Trans. I.S.I. Jpn* **17** 21
McNallan M J and King T B 1982 *Metall. Trans.* **B13** 165
Sahai Y and Guthrie R I L 1982 *Metall. Trans.* **B13** 193
Themelis N J, Tarasoff P and Szekely J 1967 *Trans. TMS-AIME* **245** 2425